Journal of Thermal Engineering
https://jten.yildiz.edu.tr/
https://doi.org/10.47481/jten.0066

RESEARCH ARTICLE

Hydrogen enrichment in gas turbines: A CFD study on NOx reduction for sustainable energy systems

Maryam Haghjou[1,*], Mohammad Javadzadeh[2]

[1]Department of Agricultural Economics, Faculty of Agriculture, University of Tabriz, Tabriz 51666-16471, Iran
[2]Department of Mechanical Engineering, National Iranian Gas Company (NIGC), Tabriz 4694-11365, Iran

Abstract

Nitrogen oxides (NOx) emissions from gas turbines, resulting from high-temperature combustion, pose significant environmental and health challenges, needing innovative strategies for sustainable energy production. This computational fluid dynamics (CFD) study investigates the efficacy of hydrogen enrichment (0–30% by mass) and inlet air/fuel temperature variations in reducing NOx emissions in a single-can reverse-flow gas turbine combustor. Implemented in ANSYS Fluent 6.3.26 with the k-ω SST turbulence model and eddy-dissipation combustion, the model employs a 507,659-cell mesh, confirmed against experimental NOx data (15–25 ppm for natural gas, simulated 27.4 ppm). Hydrogen blending reduces peak flame temperatures from 999 °C (0% H_2) to 937 °C (30% H_2), achieving a 90% NOx reduction (below 1 ppm) at 30% hydrogen due to lean combustion (equivalence ratio 0.263). Inlet air temperature increases (630–680 K) elevate NOx by 51% (20.5–31 ppm), while fuel temperature rises (260–320 K) increase NOx by 11% (27–30 ppm). Inlet cooling enhances NOx abatement without added infrastructure. The novel synergy of hydrogen enrichment and inlet cooling outperforms conventional methods like selective catalytic reduction (SCR), offering a scalable, efficient solution for sustainable turbine operation. Future thermodynamic cycle analyses are recommended to perfect system-wide performance.

Keywords: Hydrogen enrichment, NOx reduction, CFD modeling, lean combustion, gas turbine sustainability

Cite this article as: Cite this article as: Haghjou, M., & Javadzadeh, M. (2026). Hydrogen enrichment in gas turbines: A CFD study on NOx reduction for sustainable energy systems. Journal of Thermal Engineering, 12(5), 1798–1804. https://doi.org/10.47481/jten.0066

Highlights:

- Achieves 90% NOx reduction with 30% hydrogen blending.
- Inlet cooling synergistically enhances NOx abatement.
- Validated CFD model supports practical, sustainable turbine designs.
- Aligns with stringent environmental regulations.

Highlights:

- Up to 90% NOx reduction achieved with 30% hydrogen blending.
- Inlet cooling synergistically enhances NOx abatement.
- Validated CFD model supports practical, sustainable turbine designs.

1. Introduction

Nitrogen oxides (NOx), formed during high-temperature combustion in gas turbines, contribute to air pollution, acid rain, and respiratory health issues (World Health Organization, 2021; Likens et al., 1996). With global electricity demand projected to increase (International Energy Agency, 2022), gas turbines stay critical for power generation but face stringent NOx emission regulations (European Commission, 2016). Traditional mitigation strategies, such as water/steam injection (Lefebvre & Ballal, 2010), dry low-NOx (DLN) combustion (Turns, 2012), and selective catalytic reduction (SCR) (Heck & Farrauto, 2001), often involve efficiency losses, high costs, or secondary pollutants. Hydrogen enrichment offers a promising alternative, using its high flame speed and wide flammability range to enable lean combustion, reducing NOx

*Corresponding Author
E-mail Adress: m_haghjou@tabrizu.ac.ir

Submitted: 6 May 2025; **Accepted:** 26 June 2025

This paper was recommended for publication in revised form by Editor-in-Chief Ahmet Selim Dalkılıç

formation while keeping performance (Ditaranto & Mercati, 2011; Kumar et al., 2024).

Recent research highlights hydrogen's potential. TerMaath et al. (2006) reported a 50–60% NOx reduction in midsize turbines with hydrogen blends, while Lee et al. (2010) proved improved combustion stability. Nazari et al. (2022) achieved a 25% NOx reduction with 20% hydrogen, emphasizing combustion tuning. Moon et al. (2022) reduced NOx by 50% in lean-premixed systems, though higher hydrogen fractions introduced instabilities. Pashchenko (2023) showed that steam injection with hydrogen cut NOx by 35%, and Maka and Mehmood (2024) confirmed low-NOx performance in 12 MW green hydrogen turbines. However, gaps stay in quantifying the combined effects of hydrogen fractions and inlet temperature control in single-can reverse-flow combustors under realistic conditions. Prior studies often overlook inlet cooling's role or focus on specific hydrogen fractions, limiting practical applicability (Chacartegui et al., 2011; Al-Gebory, 2019, Kumar et al., 2022).

Objective and Novelty: This study employs CFD to evaluate hydrogen enrichment (0–30% by mass) and inlet air/fuel temperature effects on NOx emissions in a single-can reverse-flow gas turbine combustor, as shown in Figure 1. The novelty lies in proving a synergistic hydrogen-cooling strategy that achieves up to 90% NOx reduction without hardware modifications, surpassing conventional methods in efficiency and sustainability.

2. Combustion system description

2.1. Combustion chamber

The single-can reverse-flow combustor, flanged to the high-pressure turbine casing, forms an outer shell, fuel nozzle, liner, and spark plug, as illustrated in Figure 1. Compressor air enters counter to the combustion gas flow, divided into primary (combustion), secondary (dilution), and cooling streams to perfect flame stability and temperature control, critical for NOx reduction.

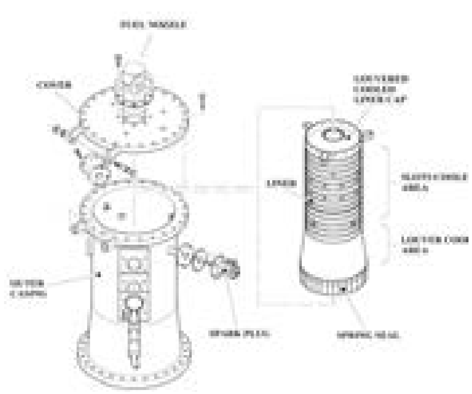

Figure 1. Combustion chamber assembly, showing primary and secondary air inlets, fuel nozzle, liner, and exhaust flow path

2.2. Liner

The reverse-flow liner, constructed from a nickel-based superalloy, features a cylindrical midsection and conical end. Its slotted and louvered cooling system mitigates thermal loads, supporting efficient hydrogen-blended combustion.

2.3. Fuel nozzle

The fuel nozzle, with eight orifices angled at 45 degrees, induces swirling flow for enhanced fuel-air mixing, using hydrogen's combustion properties to minimize NOx formation.

3. Geometry, boundary conditions, mesh, and numerical method

3.1. Problem specifications

The computational domain extends from the compressor discharge to the combustion chamber exit, with a length of 1300 mm and an outer diameter of 700 mm, as shown in Figure 2. The single-can reverse-flow combustor features a centrally positioned fuel nozzle and a perforated liner for air entry. Air mass flow is fixed at 46.67 kg/s, with fuel compositions varying as specified in Table 2. Inlet air temperatures range from 630 K to 680 K, reflecting typical compressor discharge conditions in industrial gas turbines (Boyce, 2006). Fuel inlet temperatures (260–320 K) align with pipeline gas conditions post-pressure regulation, ensuring practical relevance.

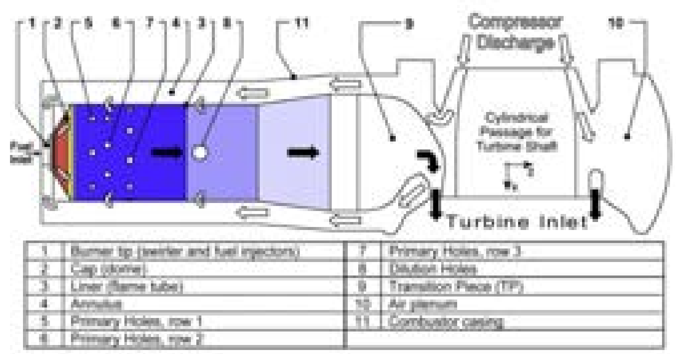

Figure 2. Longitudinal section of the combustion chamber, highlighting primary/secondary air inlets and fuel nozzle

3.2. Boundary conditions, mesh, and numerical method

The CFD model, implemented in ANSYS Fluent 6.3.26, uses a 507,659-cell mesh (183,215 cells, 387,404 faces, 41,359 nodes) to ensure grid-independent results, as shown in Figures 3 and 4. Adiabatic boundaries and steel surfaces simulate realistic conditions. The k-ω SST turbulence model (Menter et al., 2003) was selected for its accuracy in jet flows and near-wall effects, confirmed against Behnia et al. (1999). The eddy-dissipation combustion model captures turbulent-chemistry interactions, and thermal NOx is tracked via the Extended Zeldovich mechanism (Hanson & Salimian, 1984). Convergence is achieved at a 10^{-6} residual criterion. Temperature ranges were chosen based on industrial turbine data (Boyce, 2006).

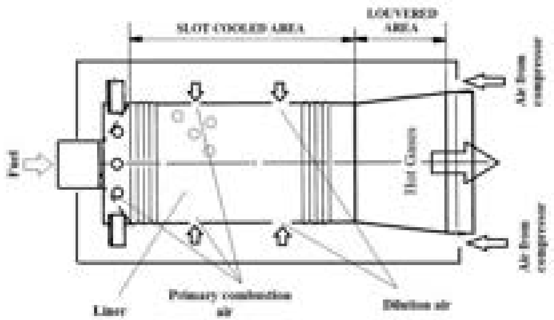

Figure 3. Grid independence study using axial velocity along the symmetry axis from the fuel nozzle outlet, showing convergence across mesh sizes

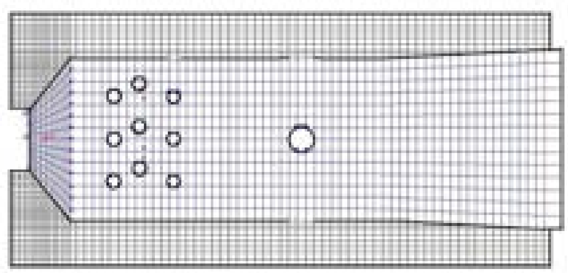

Figure 4. Computational domain and mesh at the combustion chamber's longitudinal section, with finer cells near the fuel nozzle and air inlets

3.3. Geometry and mesh

The mesh was generated using Gambit 2.2, with four sizes (65,548, 187,282, 355,835, and 507,659 cells) evaluated for grid independence, as shown in Figure 5. The 507,659-cell mesh was selected for its reliable results. Finer cells near the fuel nozzle and air entry holes capture steep gradients, while coarser cells at air inlets reduce computational cost, as depicted in Figure 6.

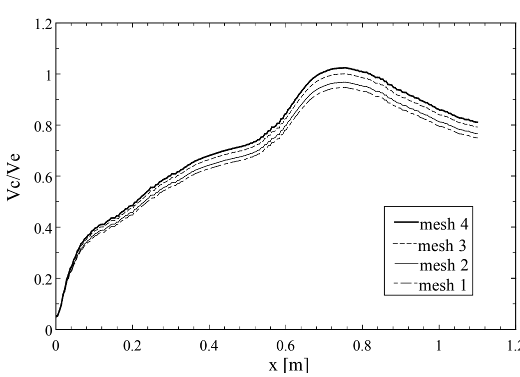

Figure 5. Grid independence study using normalized axial velocity along the symmetry axis from the fuel nozzle outlet

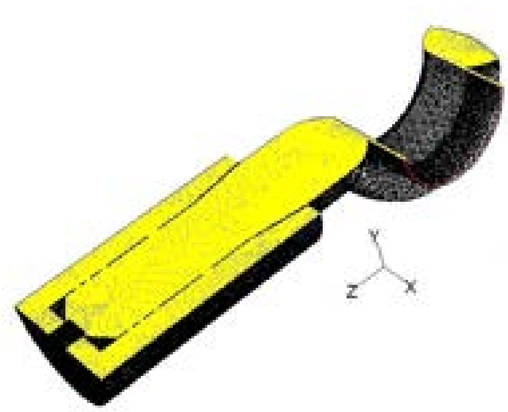

Figure 6. Detailed mesh at the combustion chamber's symmetry plane, showing cell distribution

3.4. Governing physics

The fluid flow is modeled as an ideal gas, solving conservation equations as follows (Borman & Ragland, 1998):

$$\frac{\partial \rho}{\partial t} + \frac{\partial (\rho . u_i)}{x_i} = 0 \quad (1)$$

$$\rho \frac{Du_j}{Dt} = \rho . \left(\frac{\partial u_j}{\partial t} + u_i \frac{\partial u_j}{\partial x_i} \right) = \frac{\partial p}{\partial x_j} + \frac{\partial \tau_{ij}}{\partial x_i} + f_i \quad (2)$$

$$\tau_{ij} = \mu \left(\frac{\partial u_i}{\partial x_j} + \frac{\partial u_j}{\partial x_i} \right) - \delta_{ij} \frac{2}{3} \mu \frac{\partial u_i}{\partial x_i} \quad (3)$$

$$\rho \frac{D}{Dt} \left(e + \frac{p}{\rho} \right) = \rho \frac{Dh}{Dt} = \frac{Dp}{Dt} + \nabla . (k . \nabla T) + \mu \varphi \quad (4)$$

The k-ω SST turbulence model governs turbulent flow (Menter et al., 2003):

$$a_1 CH_4 + a_2 C_2H_6 + a_3 C_3H_8 + a_4 C_4H_{10} + a_5 C_5H_{12} + a_6 H_2 + b.\lambda.(O_2 + 3.76N_2) \rightarrow \quad (5)$$

$$cCO_2 + dH_2O + 3.76bN_2 + eO_2 ,$$

$$b = 2a_1 + 3.5a_2 + 5a_3 + 6.5a_4 + 8a_5 + 0.5a_6 \quad (6)$$

Thermal NOx formation is modeled using the Extended Zeldovich mechanism (Hanson & Salimian, 1984):

$$c = a_1 + 2a_2 + 3a_3 + 4a_4 + 5a_5 \quad (7)$$

$$d = 2a_1 + 3a_2 + 4a_3 + 5a_4 + 6a_5 + a_6 \quad (8)$$

$$e = b.\lambda - c - \frac{d}{2} \quad (9)$$

Table 1. Gas turbine specifications (Nuovo Pignone, 1999), detailing compressor, combustor, and turbine parameters

Parameter	Specification
Axial Compressor	11-Stage Axial Flow, 15.5:1 Pressure Ratio
Combustion Chamber	Single-Can Combustor, DLN Gas Fuel at 25 ppm NOx
Turbine	2 Stages High Pressure, 2 Stages Low Pressure
Nominal Rating	15 °C, Sea Level, 60% Relative Humidity
Fuel	Natural Gas (LHV = 32–44 MJ/Nm^3)
Electrical Output	11,982 kW
Electrical Efficiency	33.3%
Exhaust Flow	47.0 kg/s

Table 2. Natural gas/Hydrogen fuel composition (mass fractions), specifying fuel blends for cases 1–4

Fuel Composition	Case 1 (Natural Gas)	Case 2	Case 3	Case 4
CH_4	0.896	0.851	0.802	0.760
C_2H_6	0.063	0.060	0.056	0.054
C_3H_8	0.031	0.030	0.028	0.027
C_4H_{10}	0.007	0.006	0.006	0.006
C_5H_{12}	0.003	0.003	0.003	0.003
H_2	0.000	0.050	0.104	0.151

Table 3. Computational specifications for combustion simulation, outlining hardware and simulation time

Parameter	Specification
Processor	Intel Core i7, 3.5 GHz
RAM	16 GB
Simulation Time	~6 hours

4. Mixture studies

Fuel blends keep constant energy input, with hydrogen fractions increasing from 0% to 30%. The combustion reaction is modeled as (Borman & Ragland, 1998):

$$(q_{lhv} \cdot \dot{m})_{Naturalgas} = (q_{lhv,Naturalgas} \cdot \dot{m}_{Naturalgas} + q_{lhv,H2} \cdot \dot{m}_{H2}) \quad (10)$$

Energy consistency is ensured by (Borman & Ragland, 1998):

$$\frac{\partial}{\partial t}(\rho k) + \frac{\partial}{\partial x_i}(\rho \cdot k \cdot u_i) = \frac{\partial}{\partial x_j}\left(\Gamma_k \frac{\partial k}{\partial x_j}\right) + \widetilde{G}_k - Y_k + S_k \quad (11)$$

$$\frac{\partial}{\partial t}(\rho \omega) + \frac{\partial}{\partial x_i}(\rho \cdot \omega \cdot u_i) = \frac{\partial}{\partial x_j}\left(\Gamma_\omega \frac{\partial \omega}{\partial x_j}\right) + \widetilde{G}_\omega - Y_\omega + D_\omega + S_\omega \quad (12)$$

5. Results and discussion

5.1. Validation and initial findings

The CFD model predicts 27.4 ppm NOx for natural gas, aligning with experimental data (15–25 ppm, Nuovo Pignone, 1999), with a 7% overprediction due to omitted radiation effects (Behnia et al., 1999). Hydrogen fractions (0–30%) and inlet temperatures were analyzed, as detailed in Table 2.

5.2. Velocity, temperature, and NOx contours

Velocity contours (Figure 7) show high magnitudes near the fuel nozzle and air inlets, decreasing toward the exit with a stagnation point. Temperature contours (Figure 8) show peak temperatures in the central flame zone, moderated by secondary air. NOx contours (Figure 9) reflect thermal NOx's temperature dependence, increasing downstream.

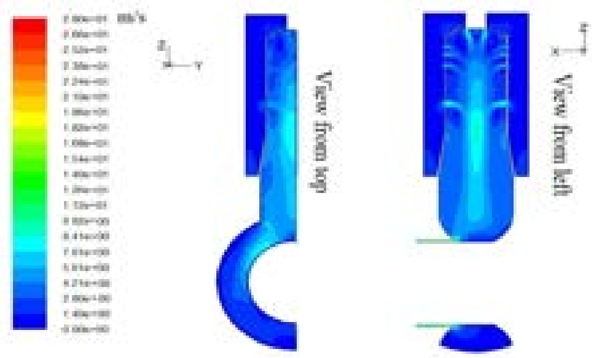

Figure 7. Velocity contours (front and top views) show high velocities near the fuel nozzle and air inlets due to inlet momentum, decreasing toward the chamber exit with a stagnation point

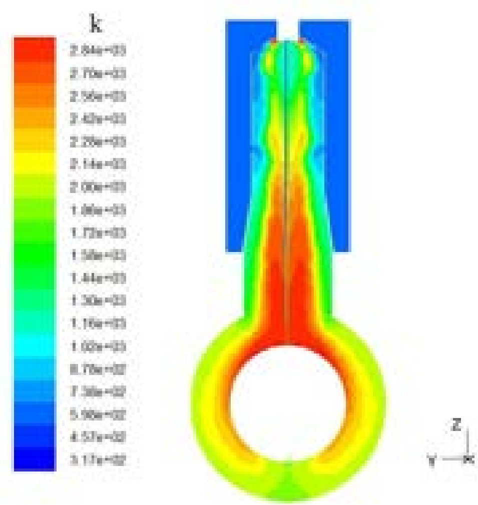

Figure 8. Temperature contours indicate pshoweratures in the central flame zone, moderated by secondary air injection to protect turbine blades

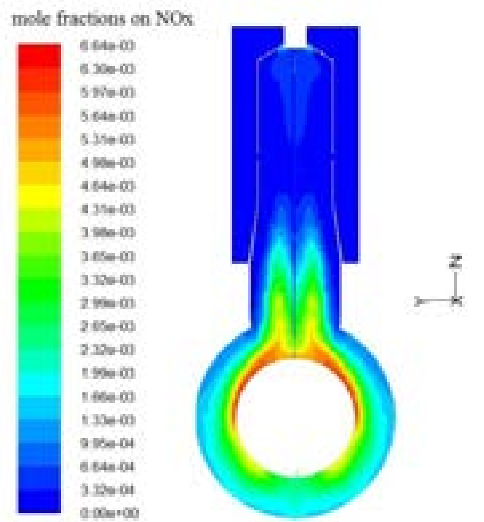

Figure 9. NOx contours reflect the temperature dependence of thermal NOx, with minimal levels near the nozzle and increases due to elevated gas temperatures

5.3. Temperature distribution

Hydrogen reduces peak flame temperatures from 999 °C (0% H_2) to 937 °C (30% H_2), as shown in Figure 10, due to leaner combustion (Choudhuri & Gollahalli, 2000).

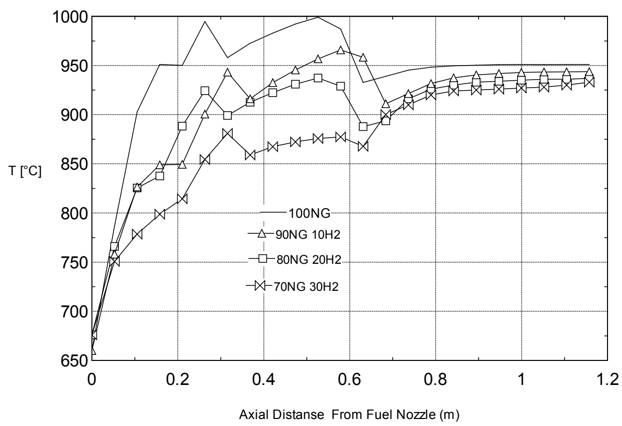

Figure 10. Axial temperature distribution along the combustion chamber for various fuel compositions, showing temperature reduction with hydrogen

5.4. NOx concentration

NOx emissions drop to 6–7 ppm at 10% H_2 and below 1 ppm at 30% H_2 (Figure 11), a 90% reduction driven by lean combustion (Hanson & Salimian, 1984).

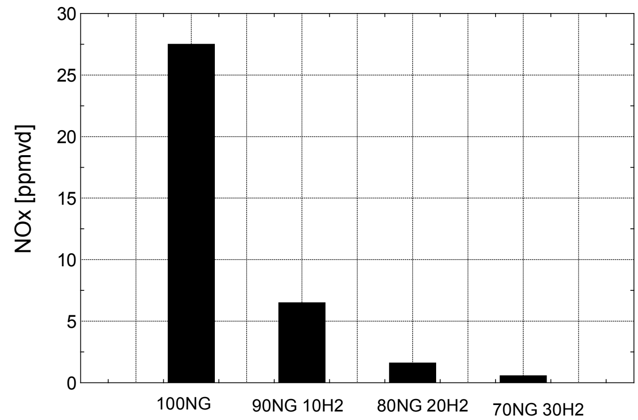

Figure 11. NOx emissions for various hydrogen fractions, proving up to 90% reduction

5.5. Effect of inlet air temperature

Inlet air temperature increases from 630 K to 680 K raise NOx by 51% (20.5–31 ppm), as shown in Figure 12, due to enhanced thermal NOx formation (Cengel & Boles, 1998).

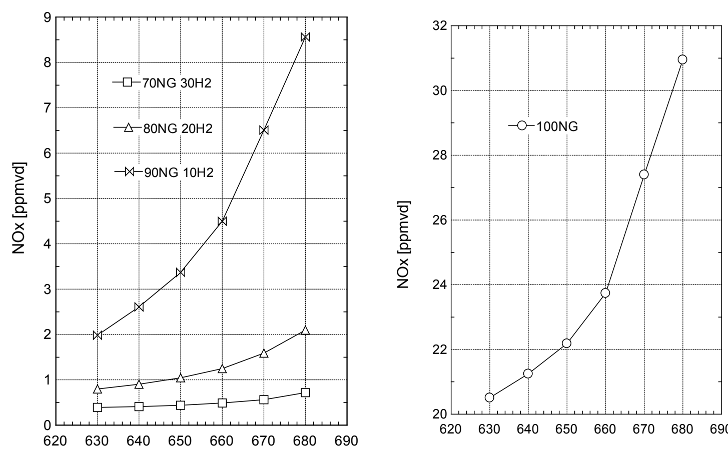

Figure 12. Effect of inlet air temperature on NOx emissions for various fuel compositions

5.6. Effect of inlet fuel temperature

Fuel temperature rises from 260 K to 320 K increase NOx by 11% (27–30 ppm), while cooling to 260 K reduces it to 24 ppm (Figure 13), using pressure regulation (Kamal & Gollahalli, 2001).

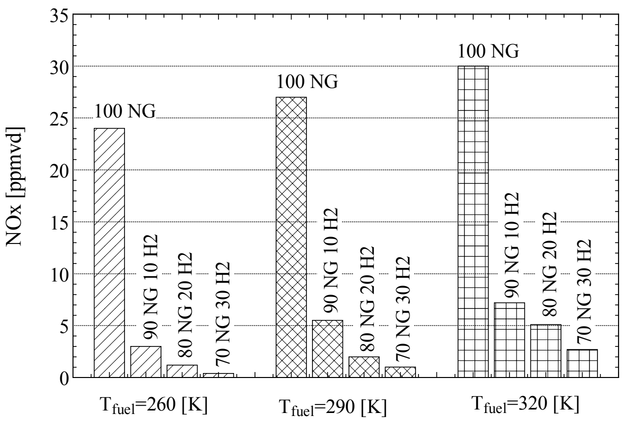

Figure 13. Effect of inlet fuel temperature on NOx emissions, highlighting benefits of fuel cooling

5.7. Practical implications

A 10% H_2 blend offers a "drop-in" solution (75% NOx reduction), while 30% H_2 achieves near-zero NOx but requires combustor modifications. Inlet cooling enhances reductions without infrastructure changes (Boyce, 2006).

6. Conclusion

This study proves the synergistic potential of hydrogen enrichment and inlet temperature control in reducing NOx emissions from gas turbines, offering a sustainable pathway for cleaner energy production. Hydrogen addition up to 30% by mass reduces NOx below 1 ppm, outperforming traditional methods like water injection or SCR, which often compromise efficiency or introduce secondary pollutants. Inlet air cooling further enhances this reduction by using thermal dynamics, aligning turbine operations with stringent air quality standards and global sustainability goals. This approach mitigates smog, acid rain, and health risks without requiring extensive infrastructure changes. As fossil fuel reliance diminishes, hydrogen appears as a pivotal element in decarbonizing gas turbines. Future research could explore higher hydrogen fractions and advanced cooling techniques to further perfect this strategy, solidifying gas turbines' role in a sustainable energy future.

Key findings include:

- Hydrogen addition reduces combustion chamber temperatures.
- It lowers the equivalence ratio, leading to leaner mixtures, reduced temperatures, and thus lower NOx.
- A 10% hydrogen blend achieves a 75% NOx reduction, with 30% being optimal for maximum abatement.
- Higher inlet air temperatures increase combustion product temperatures and NOx via the Zeldovich mechanism.
- Elevated fuel inlet temperatures similarly increase NOx production.

Notably, fuel is sourced from a main gas pipeline, regulated to reduce pressure and temperature (by ~15 °C), negating the need for added cooling equipment. While CFD effectively analyzes velocity, temperature, and NOx distributions, it cannot assess broader cycle impacts, suggesting thermodynamic modeling for comprehensive evaluation, as planned for future work.

6.1. Future recommendations

- Investigate higher H_2 fractions for scalability.
- Develop advanced cooling systems.
- Conduct cycle-wide efficiency analyses.

Author contributions statement

Maryam Haghjou: Conceptualization; Methodology; Software; Validation; Formal Analysis; Investigation; Data Curation; Writing – Original Draft Preparation; Writing – Review & Editing; Visualization; Project Administration. Mohammad Javadzadeh: Conceptualization; Methodology; Software; Formal Analysis; Investigation; Data Curation; Writing – Review & Editing; Supervision; Resources. All authors have read, reviewed, and approved the final version of the manuscript and agree to be accountable for all aspects of this work.

Declaration of interests

The authors declare that they have no known competing financial interests or personal relationships that could have appeared to influence the work reported in this paper. This research was conducted independently without any commercial or organizational support that could be construed as a potential conflict of interest.

Data availability

The data that support the findings of this study are available from the corresponding author upon reasonable request. The CFD model geometry, boundary conditions, and solver settings are fully described in the manuscript to ensure reproducibility. Due to the proprietary nature of the industrial gas turbine geometry, the raw CAD data are not publicly available; however, all relevant simulation parameters and results are presented in sufficient detail to enable independent verification.

Declaration of generative AI and AI-assisted technologies in the writing process

During the preparation of this manuscript, the authors used AI-assisted language tools exclusively for native-level English language editing and linguistic polishing of the written text. No generative AI was used for any aspect of scientific research, including conceptualization, method, simulation execution, data analysis, interpretation of results, or drawing of conclusions. All simulations and analyses were performed entirely by the authors, and the AI-assisted editing was applied solely after the scientific content was fully developed and verified. The authors take full responsibility for the integrity and originality of all content presented in this paper.

References

[1] Al Gebory, L (2019). Participation Media for Volumetric Heat Generation. Journal of Thermal Engineering, 5(1), 39-99. 10.18186/thermal.505495

[2] Behnia, M., et al. (1999). International Journal of Heat and Fluid Flow, 20(1), 1–9. https://doi.org/10.1016/S0142-727X(98)10043-7

[3] Borman, G. L., & Ragland, K. W. (1998). Combustion Engineering. McGraw-Hill.

[4] Boyce, M. P. (2006). Gas Turbine Engineering Handbook (3rd ed.). Gulf Professional Publishing.

[5] Cengel, Y. A., & Boles, M. A. (1998). Thermodynamics: An Engineering Approach (3rd ed.). McGraw-Hill.

[6] Chacartegui, R., et al. (2011). Fuel Processing Technology, 92(2), 213–220. https://doi.org/10.1016/j.fuproc.2010.09.030

[7] Choudhuri, A. R., & Gollahalli, S. R. (2000). International Journal of Hydrogen Energy, 25(5), 451–462. https://doi.org/10.1016/S0360-3199(99)00047-2

[8] Ditaranto, M., & Mercati, S. (2011). Energy Procedia, 4, 2053–2060. https://doi.org/10.1016/j.egypro.2011.02.087

[9] European Commission. (2016). Official Journal of the European Union, L 344, 1–31. https://eur-lex.europa.eu/eli/dir/2016/2284/oj

[10] Elmeriah, A, Sandid, A, Taeib, Nehri, D & Chouli, F (2026). Computational fluid dynamics study (CFD) of cooling systems heat transfer fluids (HTFS) for electrical cabins . Journal of Thermal Engineering, 12(4):1480-1492. DOI: 10.47481/jten.0045

[11] Hanson, R. K., & Salimian, S. (1984). In Combustion Chemistry (pp. 361–421). Springer.

[12] Heck, R. M., & Farrauto, R. J. (2001). Catalytic Air Pollution Control (2nd ed.). Wiley.

[13] International Energy Agency. (2022). World Energy Outlook 2022. https://www.iea.org/reports/world-energy-outlook-2022

[14] Kamal, A., & Gollahalli, S. (2001). Journal of Energy Resources Technology, 123(2), 167–170. https://doi.org/10.1115/1.1367858

[15] Kumar, K. S., et al. (2022). International Journal of Ambient Energy, 43(1), 8577–8591. https://doi.org/10.1080/01430750.2022.2075932

[16] Kumar, K. S., et al. (2024). Journal of Cleaner Production, 434, 140354. https://doi.org/10.1016/j.jclepro.2023.140354

[17] Lee, M. C., et al. (2010). Fuel, 89(7), 1485–1491. https://doi.org/10.1016/j.fuel.2009.10.004

[18] Lefebvre, A. H., & Ballal, D. R. (2010). Gas Turbine Combustion (3rd ed.). CRC Press.

[19] Likens, G. E., et al. (1996). Science, 272(5269), 244–246. https://doi.org/10.1126/science.272.5269.244

[20] Maka, A. O. M., & Mehmood, M. (2024). Clean Energy, 8(2), 1–7. https://doi.org/10.1093/ce/zkae012

[21] Menter, F. R., et al. (2003). Turbulence, Heat and Mass Transfer 4, 625–632.

[22] Moon, K., et al. (2022). Combustion and Flame, 235, 111697. https://doi.org/10.1016/j.combustflame.2021.111697

[23] Nazari, M. A., et al. (2022). International Journal of Low-Carbon Technologies, 17, 513–519. https://doi.org/10.1093/ijlct/ctac025

[24] Nuovo Pignone S.p.A. (1999). http://www.ge.com/oilandgas/

[25] Pashchenko, D. (2023). Renewable and Sustainable Energy Reviews, 173, 113117. https://doi.org/10.1016/j.rser.2022.113117

[26] TerMaath, C. Y., et al. (2006). International Journal of Hydrogen Energy, 31(8), 1147–1158. https://doi.org/10.1016/j.ijhydene.2005.10.005

[27] Turns, S. R. (2012). An Introduction to Combustion (3rd ed.). McGraw-Hill.

[28] World Health Organization. (2021). https://www.who.int/publications/i/item/9789240034228